Josephson Effect for Photons in Two Weakly Linked Microcavities

An-Chun Ji,[1,2] Qing Sun,[1] X. C. Xie,[3,1] and W. M. Liu[1]

[1]*Beijing National Laboratory for Condensed Matter Physics, Institute of Physics, Chinese Academy of Sciences,*
Beijing 100190, China
[2]*Department of Physics, Capital Normal University, Beijing 100048, China*
[3]*Department of Physics, Oklahoma State University, Stillwater, Oklahoma 74078, USA*
(Received 7 October 2008; published 15 January 2009)

We describe an optical system that allows for direct observation of the photonic Josephson effects in two weakly linked microcavities containing ultracold two-level atoms. We show that, by moving the ultracold atoms within one cavity, we could simulate an analogous superconducting circuit and realize both the alternating- and direct-current (ac and dc) photonic Josephson effects. This provides a strategy for constructing novel interference devices of coherent photons and enables new investigations of the effect of many-body physics in strongly coupled atom-cavity systems.

The strongly correlated dynamics of coherent photons has achieved many exciting experimental and theoretical advances such as effective photon-photon repulsion [1], the Mott insulator-superfluid quantum phase transition of light [2], simulations of the quantum magnetic dynamics of spin models [3], and quantum magnetic dynamics of polarized light in arrays of microcavities [4]. Compared to other strongly correlated many-particle systems in condensed matter physics or cold atoms, an optical correlation system has the advantage of accessing individual lattices experimentally [5]. In addition, it offers the ability to design quantum-mechanical devices for quantum information processes.

In this Letter, we explore the photonic Josephson effects of a strongly interacting many-body optical system where the polaritons condense into a superfluid quantum phase. The wave function of this phase is a superposition of the coherent states of photons and two-level atoms [6]. When the freedom of the atom polarization is integrated out, the superfluid phase can be described by the order parameter of the photon wave function via an effective field theory [7]. These coherent photons are novel quasiparticles that are self-interacting and behave like massive bosons; thus, they can serve as good candidates for the quantum simulations of the correlation effects in condensed matter physics.

In real experiments, the striking signatures of the Josephson effects are demonstrated by measuring the chemical potential-current relation of the ac and dc Josephson effects [8]. This is analogous to the voltage-current characteristic in a superconducting Josephson junction biased by external circuits [9]. But in charge-neutral systems such as atomic Bose-Einstein condensates (BECs), where the external circuits and current sources are absent, it is very difficult to implement the chemical potential-current relation [10]. Here we set up an optical correlation system consisting of two weakly linked microcavities with ultracold atoms within each cavity. We show that, by moving the atoms in a modulated local atom field,

we can realize a time-dependent coupling between the moving atoms and cavity photons; thus, a biased photonic current could be applied. This technique, for the first time, provides a practical way to explore the photonic Josephson effects, which play important roles for understanding the temporal interference of coherent photons.

The system under investigation is schematically depicted in Fig. 1(a). We have considered two fiber-based Fabry-Perot (FFP) or ultrahigh-finesse optical cavities [11,12], which can achieve the strong coupling regime with large single-atom peak coupling rate g_0 and a small rate of decay of the cavity field κ. The two cavities are linked with the intercavity tunneling amplitude $\mathcal{K}$, and each cavity contains $N^a = 10^4$ two-level ^{87}Rb atoms trapped by an external magnetic potential or dipole beam. We choose the relevant parameters $g_0/2\pi = 215$ MHz [11] and $(\kappa, \gamma)/2\pi = (1.3, 3.0)$ MHz [12]. The corresponding characteristic time scales of these parameters will be further discussed later. In Fig. 1(b), a far-detuned optical lattice is switched on to increase the atomic confinement and gain control over the coupling rate, where the period of the overlap between the cavity mode and the optical lattice is 6.4 μm [12]. By moving the ultracold atoms within the cavity, one can realize a tunable coupling rate, which is crucial for an experimental realization of the dc photonic Josephson effects. Figure 1(c) shows the modulated local atom-field coupling rate $g(x)$, where $g^2(x) = \int \frac{\rho(\mathbf{r})}{N^a} |g_0 \cos(2\pi x/\lambda_C) \exp(-r_\perp^2/w^2)|^2 d\mathbf{r}$, with w and λ_C being the mode radius and wavelength.

The Hamiltonian for our Josephson coupled atom-field interaction system can be described by a combination of the Dicke Hamiltonian [13] with photon tunneling between two weakly linked microcavities. In the rotating-wave approximation, the many-body dynamics of the full system is given by the following Hamiltonian:

$$\hat{H} = \sum_{i=1,2} \hat{H}_i^{\mathrm{D}} + \mathcal{K}(\hat{\psi}_1^\dagger \hat{\psi}_2 + \mathrm{H.c.}), \qquad (1)$$

a

FFP1 g FFP2

κ ~~~~ γ $\mathcal{K}$ $\mathcal{K}$ γ ~~~~ κ
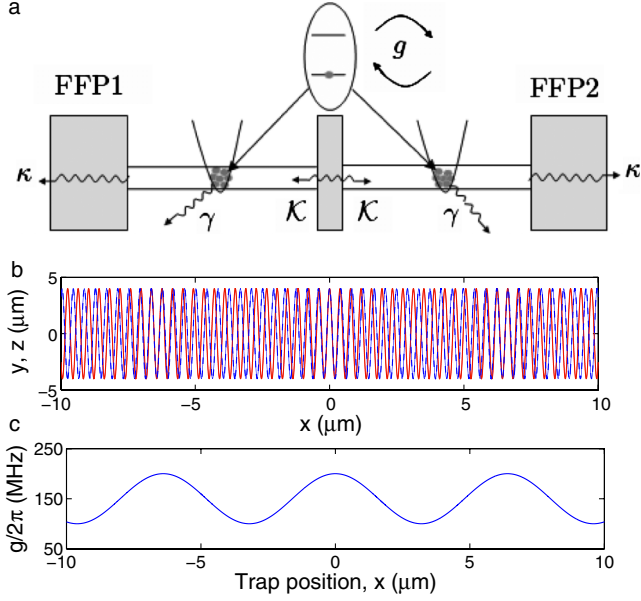
b

c

FIG. 1 (color online). Experimental setup and control of the coupling along the resonator axis. (a) Two FFP cavities are linked with a intercavity tunneling amplitude $\mathcal{K}$. Each cavity contains N^a two-level ^{87}Rb atoms trapped by an external magnetic potential or dipole beam. g is the coherent coupling rate between an individual atom and the cavity field; γ and κ are the dissipation rate of the atomic spontaneous emission and the cavity field itself, respectively. (b) The atoms are placed at a position x along the cavity axis and are loaded into the optical lattice. The cavity mode ($\lambda_C = 780$ nm) and far-detuned optical lattice ($\lambda_L = 830$ nm) standing waves in each cavity have a variable overlap with a 6.4 μm period. (c) The loaded atoms show a strongly modulated coupling depending on the local overlap between lattice and cavity mode.

$$\hat{H}_i^D = \omega_C \hat{\psi}_i^\dagger \hat{\psi}_i + \sum_{j=1}^{N^a} \frac{\omega_A}{2} (\hat{b}_{i,j}^\dagger \hat{b}_{i,j} - \hat{a}_{i,j}^\dagger \hat{a}_{i,j})$$
$$+ g_i(\hat{b}_{i,j}^\dagger \hat{a}_{i,j} \hat{\psi}_i + \hat{\psi}_i^\dagger \hat{a}_{i,j}^\dagger \hat{b}_{i,j}), \qquad (2)$$

where ω_C and ω_A are the cavity and atom resonance frequencies, respectively, with the detuning $\Delta_C = \omega_C - \omega_A$. $\hat{\psi}_i^\dagger$ ($\hat{\psi}_i$) is the single-mode creation (annihilation) operator of the photons in each cavity; $\hat{a}_{i,j}$ and $\hat{b}_{i,j}$ are fermion operators, which are naturally associated with the lower and upper levels of each atom and satisfy the single-occupancy constraint [7]. The modulated local atom-field coupling rate $g_i(x) \simeq 2\pi \times [50\cos(2\pi x/6.4) + 150]$ MHz. The intercavity tunneling amplitude is given by $\mathcal{K} = 2\omega_C \int d\mathbf{r}[\epsilon_i(\mathbf{r}) - \epsilon(\mathbf{r})]w_1^*(\mathbf{r})w_2(\mathbf{r})$ [3], where $\epsilon_i(\mathbf{r})$ and $w_i(\mathbf{r})$ are the dielectric function and the eigenmode of an individual single cavity, respectively, and $\epsilon(\mathbf{r})$ is the dielectric function of the coupled cavities.

We first analyze the excitations of the atom-cavity system with the Hamiltonian (2). We work in the grand-canonical ensemble $\tilde{H}_i^D = \hat{H}_i^D - \mu_i \hat{N}_i^{\text{ex}}$, with the total number of excitations fixed by $\hat{N}_i^{\text{ex}} = \sum_{j=1}^{N^a} \frac{1}{2} \times$

$(\hat{b}_{i,j}^\dagger \hat{b}_{i,j} - \hat{a}_{i,j}^\dagger \hat{a}_{i,j} + 1) + \hat{\psi}_i^\dagger \hat{\psi}_i$. By using the coherent state functional integral representation for the partition function [6,7] with single-occupancy constraint $\hat{a}_{i,j}^\dagger \hat{a}_{i,j} + \hat{b}_{i,j}^\dagger \hat{b}_{i,j} = 1$ and integrating over the fermion fields, one arrives at an effective action for photons

$$S_{\text{eff}}[\psi_i] = \int_0^\beta d\tau \psi_i^*(\partial_\tau + \tilde{\omega}_C^i)\psi_i - \mu_i N^a/2$$
$$- N^a \text{Tr} \ln \begin{pmatrix} \partial_\tau + \tilde{\varepsilon}_i & g_i\psi_i/\sqrt{N^a} \\ g_i\psi_i^*/\sqrt{N^a} & \partial_\tau - \tilde{\varepsilon}_i \end{pmatrix}, \quad (3)$$

where $\tilde{\omega}_C^i = \omega_C - \mu_i$ and $\tilde{\varepsilon}_i = (\omega_A - \mu_i)/2$. Making the static assumption $\psi_i(\tau) = \Psi_i$, then the free energy is written as $F_i = \ln[2\cosh(\frac{1}{2}\beta\mathcal{E}_i)]/\beta + \tilde{\omega}_C^i|\Psi_i|^2 - \mu_i N^a/2$, with $\mathcal{E}_i = \sqrt{\tilde{\varepsilon}_i^2 + g_i^2|\Psi_i|^2}$.

The mean-field equations of a polariton condensate are determined by the saddle condition $\partial F_i/\partial\Psi_i^* = 0$ combined with the excitation density constraint equation $\rho_i^{\text{ex}} = \frac{1}{\beta N^a} \frac{\partial F_i}{\partial\mu_i}$, which read

$$\tilde{\omega}_C^{\,i}\Psi_i = g_i^2 N^a \frac{\Psi_i}{2\mathcal{E}_i}, \qquad \rho_i^{\text{ex}} - \frac{1}{2} = \frac{|\Psi_i|^2}{N^a} - \frac{\tilde{\varepsilon}_i}{2\mathcal{E}_i}. \quad (4)$$

Here we have let $\beta \to \infty$ and considered only the zero-temperature excitations of the system, with the ground state energy of the Hamiltonian (2) given by $E_i = \tilde{\omega}_C^i|\Psi_i|^2 - N^a\mathcal{E}_i - \mu_i N^a/2$.

When the atoms are placed at a position of the cavity with a fixed coupling rate g, the chemical potential μ and the coherent field amplitude Ψ of the system are then dependent on the excitation density ρ^{ex} and detuning Δ_C. For the atomic resonance ($\Delta_C = 0$) and low excitation density ($\rho^{\text{ex}} < 0.5$), there exists an important feature of the above Eqs. (4): The photon occupancy density $\rho = |\Psi|^2/N^a$ is linearly dependent on the excitation density
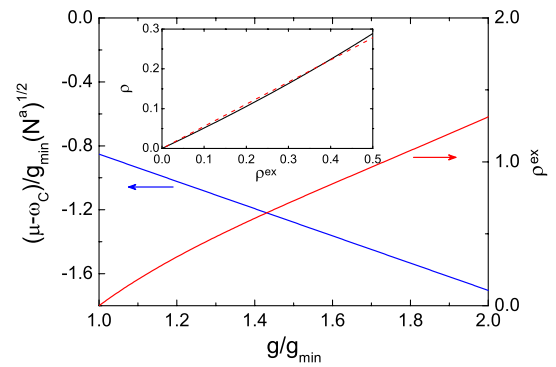

FIG. 2 (color online). Excitations of a polariton condensate. This diagram shows the dependence of excitation density ρ^{ex} on the coupling rate g for chemical potential $(\mu - \omega_C)/g_{\text{min}}\sqrt{N^a} = -1$ (red line) and the chemical potential as a function of g for the excitation density $\rho^{\text{ex}} = 0.3$ (blue line). The inset shows the photon occupancy density ρ as a function of the excitation density ρ^{ex} for atomic resonance ($\Delta_C = 0$), where the red dashed line is the linear fitting.

approximately (see the inset in Fig. 2). The linear relation can keep constant the total number of the coherent photons of two weakly linked polariton condensates. This will be beneficial when we consider the photonic tunneling between two cavities.

Moreover, we have switched on a far-detuned optical lattice to modulate the atom-field coupling rate [see Fig. 1(b)]. The atoms feel a tunable coupling rate $g(x)$ while moving along the cavity axis, resulting in variable excitations in the atom-cavity system. Figure 2 shows the dependence of excitation density ρ^{ex} on the coupling rate g for $(\mu - \omega_C)/g_{\min}\sqrt{N^a} = -1$ and the chemical potential as a function of g for $\rho^{\text{ex}} = 0.3$. We see that the excitations are determined by the tunable coupling rate, which enables an investigation of the photonic Josephson effects.

Now we explore the ac and dc Josephson effects of coherent photons in the system described by the Hamiltonian (1). The two cavities are initially tuned to atomic resonance, and both polariton condensates are excited in equilibrium with a low excitation density. The macroscopic wave function of the system can then be described as $|\Psi(t)\rangle = \Psi_1(t)|1\rangle + \Psi_2(t)|2\rangle$, with $|i\rangle$ being the two base states for each polariton condensate and $\Psi_i(t) = \sqrt{N_i(t)}e^{i\theta_i(t)}$ being the complex amplitudes [14,15]. The total number of the coherent photons $N = N_1 + N_2$ is a constant, but the photon occupations $N_i(t)$ and phases $\theta_i(t)$ are time-dependent. For low density excitations, we can expand the ground state energy of each atom-cavity system to the second order of the coherent photon occupancy density. Then the dynamics of the coherent photonic tunneling is approximately described by the following effective nonlinear Schrödinger equation:

$$i\hbar \frac{\partial |\Psi(t)\rangle}{\partial t} \simeq \left[\sum_i (E_i^0 + U_i|\Psi_i|^2)|i\rangle\langle i| + \mathcal{K}(|1\rangle\langle 2|\right.$$

$$\left. + |2\rangle\langle 1|) \right] |\Psi(t)\rangle, \qquad (5)$$

where $E_i^0 = \omega_C - \mu_i - g_i/4\mathcal{A}_i$ are the zero-point energies in each cavity and $U_i = g_i/16\sqrt{N^a}\mathcal{A}_i^3$ are the effective photonic self-interactions induced by the coupling between the atoms and the photons. Here $\mathcal{A}_i = (\omega_C -$

$\mu_i)/g_i\sqrt{N^a}$ is the dimensionless chemical potential. Then from the above Eq. (5), we obtain equations of motion for the relative population $\delta(t) = [N_1(t) - N_2(t)]/N$ and relative phase $\phi(t) = \theta_2(t) - \theta_1(t)$, which read

$$\hbar \, \dot{\delta}(t) = (2E_J/N)\sqrt{1 - \delta^2(t)} \sin\phi(t), \qquad (6)$$

$$\hbar \, \dot{\phi}(t) = Fl_x(t) + \frac{NE_C}{2}\delta(t) + \frac{2E_J\delta(t)}{N\sqrt{1 - \delta^2(t)}} \cos\phi(t), \qquad (7)$$

where $E_J = N\mathcal{K}$ is the Josephson coupling energy and $E_C = U_1 + U_2$ is the capacitive energy which is almost a constant. $l_x(t)$ describes the motion of the atoms in one of the cavities, and $F = \sqrt{N^a}(\rho^{\text{ex}}/2\mathcal{A}^3 - 1/2\mathcal{A})dg/dx$ is the average force exerted by the external trap on single atoms which generates the chemical potential difference $Fl_x(t)$ between the two cavities. Here both of the polariton condensates are initially excited with the same dimensionless chemical potential $\mathcal{A}$ in each cavity.

We confine ourselves to the Josephson regime ($E_C \gg E_J$) and consider a small population imbalance ($\delta \ll 1$). In this case, Eq. (6) is reduced to the atomic current-phase relation $\dot{\delta} \simeq \omega_J \sin\phi$, with the critical photonic current given by $\omega_J = 2E_J/\hbar N$. Then combined with Eq. (7), one arrives at the driven pendulum phase equation $\ddot{\phi} = \omega_p^2(\sin\phi + v/v_c)$, where $\omega_p = \sqrt{E_J E_C}/\hbar$ is the Josephson plasma frequency and $v_c = \hbar\omega_p^2/F$ is the critical velocity. Further, for condensates in the Josephson regime, the phase evolution equation $\dot{\phi} = -\Delta\mu/\hbar$ applies, with $\Delta\mu = \mu_1 - \mu_2$ the chemical potential difference. One then derives an analogous superconducting circuit [10]

$$\omega_J \sin\phi + G\Delta\mu + \triangle\dot{\mu}/(NE_C/2) = \dot{\delta}_{\text{equil}}, \qquad (8)$$

where $\dot{\delta}_{\text{equil}} = \omega_J v/v_c$ is the applied photonic current bias and δ_{equil} is the equilibrium value of the relative population. G is the conductance due to the noncoherent photons, which is negligible during the characteristic time scale of the cavity coherent process. Finally, combined with the atomic current-phase relation, the chemical potential difference is then associated with the population imbalance
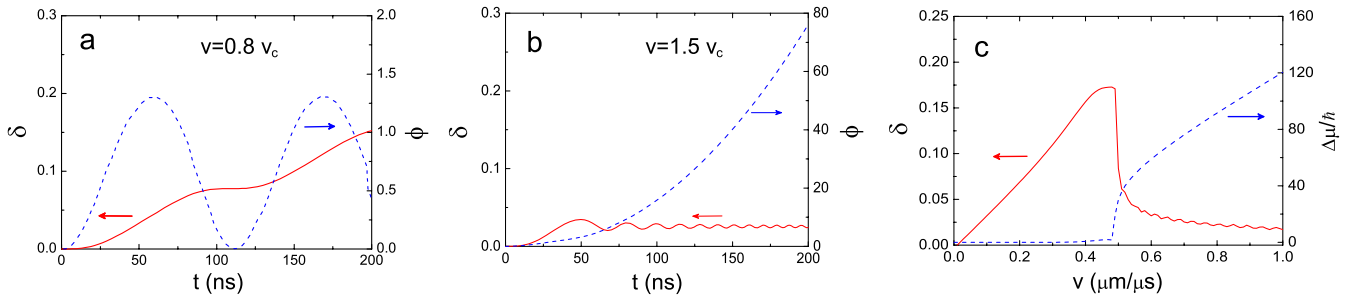

FIG. 3 (color online).   The chemical potential-current relation in the polariton condensates. (a),(b) Time evolution of the relative population (solid line) and phase (dashed line) for (a) $v = 0.8v_c$ and (b) $v = 1.5v_c$. (c) Dependence of the relative population (solid line) and the chemical potential difference (dashed line) on the velocity of the moving optical lattice. This diagram shows that there exists a sharp transition with the critical velocity $v_c = 0.48 \ \mu\text{m}/\mu\text{s}$.

$\Delta\mu = \frac{NE_C}{2}(\delta - \delta_{\text{equil}})$. This relation can be used to measure the chemical potential difference between two cavity polariton condensates in experiments.

To perform the chemical potential-current relation in the polariton condensates, we solve Eqs. (6) and (7) numerically, and the results are shown in Fig. 3. Initially, the atoms in each cavity are positioned at $x = 1.6\ \mu$m, and both of the polariton condensates are excited at a density $\rho^{\text{ex}} = 0.3$. The corresponding values of the energy parameters are $E_C N/\hbar = 7.06$ ns^{-1} and $E_J/N\hbar = 6.29 \times 10^{-4}$ ns^{-1} with the intercavity tunneling amplitude $\mathcal{K} = 2\pi \times 0.1$ MHz. Then the atoms in one of the cavities are moved at a constant velocity with the average force $F = 6.6$ ns$^{-1}\ \mu$m^{-1}, and we finally observe the population imbalance between two cavities at $t_f = 200$ ns.

The dependence of the relative population and the chemical potential difference on the velocity of the moving optical lattice is shown in Fig. 3(c), which exhibits a sharp transition at $v_c = 0.48\ \mu$m/μs. Below the critical velocity, a finite photonic current source $\dot{\delta}_{\text{equil}}$ is applied, and the system then takes an averaged constant phase difference between two condensates; see Fig. 3(a). The chemical potential difference is proportional to the time average of $\dot{\phi}$, that is, $\Delta\mu/\hbar = \frac{1}{t_f}\int_0^{t_f}\dot{\phi}dt$, which is locked around zero in this case. Thus a constant coherent photonic current $\dot{\delta} = \dot{\delta}_{\text{equil}}$ flows through the cavities, and finally a finite population imbalance exists, which can be measured in a cavity experiment. This is the dc photonic Josephson effect. Moreover, when $v > v_c$, $\dot{\delta}_{\text{equil}}$ exceeds the critical photonic current ω_J, then the relative phase starts running, and the population imbalance remains on a low average value; see Fig. 3(b). Some photonic current flows through the capacitive paths, resulting in a finite chemical potential difference $\Delta\mu$. In this case, one can observe the ac photonic Josephson effect, i.e., the oscillations of population difference between the two cavities.

Experimentally, the dc and ac photonic Josephson effects can be observed by measuring the coherent photons transmitted from each cavity with a standard photon counting system. In our system, where the atom-field interaction is in the strong coupling regime, the dynamics of the atom-cavity system is quantum dissipative [16]. The typical time scales of the dissipations are determined by cavity photon lifetime $\tau_\kappa = 2\pi/\kappa \sim 754$ ns and atom spontaneous emission lifetime $\tau_\gamma = 2\pi/\gamma \sim 330$ ns. Here we have chosen the operation time $t_f = 200$ ns. This is within the above time scales and corresponds to a couple of plasma oscillations with period $\tau_p = 2\pi/\omega_p \sim 100$ ns.

Another aspect of our proposal that should be considered is the motion of the atoms. In each cavity, the atoms are confined in a single lattice site by ramping up a tight optical lattice. While the atoms in one of the cavities are moved by the external trap, the kinetic energy increasing rate of the atoms should be smaller than the harmonic frequency of the optical lattice; thus, the atoms could be adiabatically moved. Besides, to confine the atoms in a single lattice site, one could couple Bose-Einstein condensates of the atoms to the cavities as shown in the recent experiment [12]. The kinetic energy of the atoms can then be neglected, which is valid for the wide line condition $E_{\text{rec}} \ll \hbar\Gamma$; see the supplementary notes of [12]. Further, it was found that heating of BECs will not affect the energy spectrum of the excitation.

In summary, we have shown how to implement the quantum coherent photonic tunneling between two cavity polariton condensates. Such experiments will allow us to observe directly the ac and dc photonic Josephson effects, which are of particular significance for exploring novel phenomena of cavity quantum electrodynamics and ultra-cold atoms. Moreover, this technique may be beneficial to the realization of future quantum interference devices.

[1] K. M. Birnhaum *et al.*, Nature (London) **436**, 87 (2005).
[2] A. D. Greentree *et al.*, Nature Phys. **2**, 856 (2006).
[3] M. J. Hartmann *et al.*, Nature Phys. **2**, 849 (2006).
[4] A. C. Ji *et al.*, Phys. Rev. Lett. **99**, 183602 (2007).
[5] S. Haroche and J. M. Raimond, *Exploring the Quantum: Atoms, Cavities and Photons* (Oxford University Press, Oxford, United Kingdom, 2006).
[6] P. R. Eastham and P. B. Littlewood, Phys. Rev. B **64**, 235101 (2001).
[7] V. N. Popov and V. S. Yarunin, *Collective Effects in Quantum Statistics of Radiation and Matter* (Kluwer Academic, Dordrecht, 1988).
[8] S. Giovanazzi *et al.*, Phys. Rev. Lett. **84**, 4521 (2000).
[9] A. Barone and G. Paterno, *Physics and Applications of the Josephson Effects* (Wiley, New York, 1982).
[10] S. Levy *et al.*, Nature (London) **449**, 579 (2007).
[11] F. Brennecke *et al.*, Nature (London) **450**, 268 (2007).
[12] Y. Colombe *et al.*, Nature (London) **450**, 272 (2007).
[13] R. H. Dicke, Phys. Rev. **93**, 99 (1954).
[14] A. Smerzi *et al.*, Phys. Rev. Lett. **79**, 4950 (1997).
[15] S. Raghavan *et al.*, Phys. Rev. A **59**, 620 (1999).
[16] H. J. Kimble, in *Cavity Quantum Electrodynamics*, edited by P. R. Berman (Academic, New York, 1994).